UPPSALA
UNIVERSITET

Digital Comprehensive Summaries of Uppsala Dissertations from the Faculty of Science and Technology 612

Topology Optimization for Wave Propagation Problems

EDDIE WADBRO

ACTA
UNIVERSITATIS
UPSALIENSIS
UPPSALA
2009

ISSN 1651-6214
ISBN 978-91-554-7438-6
urn:nbn:se:uu:diva-98382

Dissertation presented at Uppsala University to be publicly examined in 2446, building 2, Lägerhyddsvägen 2, Uppsala, Friday, April 3, 2009 at 10:15 for the degree of Doctor of Philosophy. The examination will be conducted in English.

Abstract

Wadbro, E. 2009. Topology Optimization for Wave Propagation Problems. Acta Universitatis Upsaliensis. *Digital Comprehensive Summaries of Uppsala Dissertations from the Faculty of Science and Technology* 612. vi, 28 pp. Uppsala. ISBN 978-91-554-7438-6.

This thesis considers topology optimization methods for wave propagation problems. These methods make no a priori assumptions on topological properties such as the number of bodies involved in the design. The performed studies address problems from two different areas, acoustic wave propagation and microwave tomography. The final study discusses implementation aspects concerning the efficient solution of large scale material distribution problems.

Acoustic horns may be viewed as impedance transformers between the feeding waveguide and the surrounding air. Modifying the shape of an acoustic horn changes the quality of the impedance match as well as the angular distribution of the radiated waves in the far field (the directivity). This thesis presents strategies to optimize acoustic devices with respect to efficiency and directivity simultaneously. The resulting devices exhibit desired far field properties and high efficiency throughout wide frequency ranges.

In microwave tomography, microwaves illuminate an object, and measurements of the scattered electrical field are used to depict the object's conductive and dielectric properties. Microwave tomography has unique features for medical applications. However, the reconstruction problem is difficult due to strongly diffracting waves in combination with large dielectric contrasts. This thesis demonstrates a new method to perform the reconstruction using techniques originally developed for topology optimization of linearly elastic structures. Numerical experiments illustrate the method and produce good estimates of dielectric properties corresponding to biological objects.

Material distribution problems are typically cast as large (for high resolutions) nonlinear programming problems over coefficients in partial differential equations. Here, the computational power of a modern graphics processing unit (GPU) efficiently solves a pixel based material distribution problem with over 4 million unknowns using a gradient based optimality criteria method.

Keywords: Topology optimization, Design optimization, Material distribution, Wave propagation problems, Inverse problems, Acoustic devices, Medical microwave tomography, High performance computing

Eddie Wadbro, Department of Information Technology, Division of Scientific Computing, Box 337, Uppsala University, SE-75105 Uppsala, Sweden

ISSN 1651-6214
ISBN 978-91-554-7438-6
urn:nbn:se:uu:diva-98382 (http://urn.kb.se/resolve?urn=urn:nbn:se:uu:diva-98382)

List of Papers

This thesis is based on the following papers, which are referred to in the text by their Roman numerals.

I Wadbro, E., Berggren, M. (2006) Topology Optimization of an Acoustic Horn. *Computer Methods in Applied Mechanics and Engineering*, 196:420–436. doi:10.1016/j.cma.2006.05.005.

II Wadbro, E., Berggren, M. (2006) Topology Optimization of Wave Transducers. In *IUTAM Symposium on Topological Design Optimization of Structures, Machines and Materials*, M. P. Bendsøe, N. Olhoff, and O. Sigmund editors: pp 301–310.

III Wadbro, E., (2006) On the far-field properties of an acoustic horn. Technical Report 2006-042, Department of Information Technology, Uppsala University.

IV Wadbro, E., Udawalpola, R., Berggren, M. (2009) Shape and Topology Optimization of an Acoustic Horn–Lens Combination. Accepted for publication in *Journal of Computational and Applied Mathematics*.

V Wadbro, E., Berggren, M. (2008) Microwave Tomography Using Topology Optimization Techniques. *SIAM Journal on Scientific Computing*, 30(3):1613–1633. doi:10.1137/070679879.

VI Wadbro, E., Berggren, M. (2009) High Contrast Microwave Tomography Using Topology Optimization Techniques. Accepted for publication in *Journal of Computational and Applied Mathematics*.

VII Wadbro, E., (2009) Microwave Tomographic Imaging as a Sequence of Topology Optimization Problems. Accepted for publication in *Optimization and Engineering*. doi:10.1007/s11081-008-9075-x.

VIII Wadbro, E., Berggren, M. (2009) Megapixel Topology Optimization Using a Graphics Processing Unit. Accepted for publication in *SIAM Review*.

Contents

1. Introduction

The dream of any designer or engineer is to design and create the optimal system. To fulfill this dream, a first step would be to define what is meant by optimal. Optimality can refer to having the smallest energy loss, the highest expected rate of return, the most esthetically appealing design, or whatever the designer sets its mind to. This thesis examines problems where the performance can be measured. That is, the performance can be evaluated as a mathematical function, henceforth denoted the *objective function*. A design is said to be optimal if the value of the objective function is as low or high (depending on the objective) as possible. Moreover, it is assumed that the physics governing the problem can be described mathematically by a *state equation*.

For industrial designs, it is required that the final structure stays within a certain area, the *design region*, and it is also common that there are additional *constraints* limiting the choices of the designer. For example, when designing a bridge, it is desired that the structure costs as little as possible (objective) under the condition that the bridge can carry at least a prespecified load (constraint). In general, design processes are iterative. First an initial design is suggested and evaluated. After the evaluation, the design is modified and tuned, then the design is reevaluated. This process is repeated over and over until no further improvements are possible.

As computers have become increasingly powerful, computer simulations have become cost-and-time-efficient complements to traditional experiments. In design processes, computer simulations typically evaluate the performance for a given configuration. An alternative to manual tuning of the design, and a good use of computational resources, is to perform numerical design optimization. In these simulations, the geometry is parameterized, and the optimal design is sought in the parameter space. That is, the algorithm systematically evaluates the performance (the objective function) for different parameter combinations. Often the geometry is parameterized from a given *reference configuration* or *ground structure*. The choice of parameterization plays an essential role for the outcome. After all, the computer program can only exploit the chosen parameterization, and thus the resulting computed optimal designs may vary dramatically as the parameterization is changed.

Numerical design optimization comes in different flavors, depending on the choice of parameterization. Three main branches in numerical design optimization in increasing levels of generality are: *sizing optimization*, *boundary shape optimization*, and *topology optimization*. Sizing optimization is used to find the optimal thicknesses (sizes) of the parts in a structure, such as the dimensions of individual beams in a truss structure. In boundary shape optimization, geometry changes, given by boundary displacements of the reference configuration, are examined. The optimal design obtained using boundary shape optimization is topologically equivalent with the reference configuration. The most general approach is topology optimization, where the connectedness of the optimal design is determined as a part of the optimization. Many projects (for example in the car industry) use a mix of these flavors. Typically, topology optimization finds a basic design, while sizing and boundary shape optimization put the final touches on the design.

Topology optimization for continuum structures is a relatively new research area and has developed rapidly during the last two decades. The first problems considered came from structural mechanics, and the most popular problem is to minimize the compliance of a structure, that is, making it as stiff as possible for a given set of load conditions and a given maximal weight. During the last decade, much work has been focused on extending the ideas and methods used in topology optimization of structures to other applications, such as fluid flows and wave propagation. The first articles concerning topology optimization applied to wave propagation problems were by Cox and Dobson [18, 21] who applied topology optimization to maximize band gaps (that is, ranges of frequencies in which waves cannot propagate) in photonic crystals for E- and H-polarized light. The next type of wave propagation problems considered was the maximization of the transmission efficiency through different devices, like photonic waveguides [10, 20, 34], or acoustical devices [35, 60]. This thesis focuses on topology optimization for wave propagation problems and aims at making the technique as successful for this problem type as for problems within structural mechanics.

2. Topology Optimization

Topology optimization addresses the problem of determining the best distribution of material within a given region. The first topology optimization like problems to be examined concerned discrete systems, such as the design of truss structures transmitting specified loads to given points of support. Already in 1866 this problem was addressed by Culmann [19], who proposed a positioning strategy for the joints in a structure. In 1904 Michell [42] published important principles for low volume truss structures, using infinitely many infinitely thin bars, that are optimal with respect to weight. The ideas laid out by Culmann and Michell have been extended and generalized [52]. The classic book by Pontryagin *et al.* [49] introduced important principles concerning optimal processes governed by differential equations. Lions [39] presented pioneering work on optimal control for partial differential equations, which inspired research also on the closely related area of design optimization. With the introduction of computers, the development of numerical algorithms for finding the optimal design escalated. Glowinski [29] and Goodman, Kohn, & Reyna [30] demonstrate early numerical algorithms regarding topology optimization of continuum structures for model problems. In 1988, Bendsøe and Kikuchi [7] published their seminal work on topology optimization for linearly elastic continuum structures. Since then, topology optimization has been subject to intense research and is today used as a part of the design process of advanced components, for instance in the car and aeronautical industries. For some classes of problems there is commercial software, from for example Altair Engineering and FE-Design. A short introduction to topology optimization, with emphasis on the methods and techniques used in the papers forming the base for this thesis, is given in this section. Eschenauer and Olhoff [26] present a review of topology optimization of continuum structures. For an exhaustive introduction to topology optimization and a presentation of many of its applications, the interested reader is referred to the monograph [9] by Bendsøe and Sigmund.

2.1 The Material Distribution Method

The most common approach to topology optimization for continuum models is to represent the presence of material with a material indicator function α, such that $\alpha(x) = 1$ if x is a point where material is present and $\alpha(x) = 0$ otherwise. The aim is to find a discrete-valued design that maximizes the performance, that is, minimizes (or maximizes) the value of the objective function.

The state equation is here assumed to be given as a variational problem of the form

$$\begin{aligned}&\text{Find } u \in \mathcal{V} \text{ such that}\\&\qquad a_\alpha(u,v) = \ell(v), \quad \forall\, v \in \mathcal{V},\end{aligned} \tag{2.1}$$

where the *state variable* u is the physical property governed by the state equation, v is a test function, and $\mathcal{V}$ is an appropriate function space denoted the *state space*. The objective function is denoted J and the optimization problem is given by

$$\begin{aligned}\min_{\alpha\in\mathcal{U}} \quad & J(\alpha,u)\\ \text{subject to} \quad & a_\alpha(u,v) = \ell(v), \quad \forall\, v \in \mathcal{V},\\ & \text{additional constraints,}\end{aligned} \tag{2.2}$$

where $\mathcal{U}$ is the set of admissible designs. For $\mathcal{U}$ being the set of all functions α such that $\alpha(x) \in \{0,1\}$ almost everywhere in the design region Ω, the optimization problem above is a nonlinear integer programming problem. These problems are computationally expensive to solve; the seemingly simpler class of linear integer programming problems is NP-complete [46, p. 358]. Another problem with the integer formulation is that, in many cases, the problems are ill-posed in that there exist non-convergent minimizing sequences. A standard method used to clear this obstacle is to relax the problem and let α take values in a continuous range, that is $\alpha(x) \in [0,1]$ almost everywhere. However, this relaxation changes the problem significantly, as will be discussed further in the following section. For elastic structures, the relaxed material indicator function α can be interpreted as a relative density and is thus often denoted ρ.

When the optimization problem is solved on a computer, the design domain is partitioned into small chunks (*elements*). The material indicator function α is then approximated by a function $\alpha_h \in \mathcal{U}_h$. Usually, the space $\mathcal{U}_h$ consists of all functions being constant on each element. The state equation is for example discretized using the finite element method. The discretized state equation is

$$\begin{aligned}&\text{Find } u_h \in \mathcal{V}_h \text{ such that}\\&\qquad a_{h,\alpha_h}(u_h,v) = \ell_h(v_h), \quad \forall\, v_h \in \mathcal{V}_h,\end{aligned} \tag{2.3}$$

where u_h, v_h, a_h, and ℓ_h are the discretized counterparts to u, v, a, and ℓ respectively, and $\mathcal{V}_h \subset \mathcal{V}$ is the discretized state space. The discretized optimization problem reads

$$\begin{aligned}\min_{\alpha_h\in\mathcal{U}_h} \quad & J_h(\alpha_h,u_h)\\ \text{subject to} \quad & a_{h,\alpha_h}(u_h,v) = \ell_h(v_h), \quad \forall\, v_h \in \mathcal{V}_h,\\ & \text{additional constraints,}\end{aligned} \tag{2.4}$$

where J_h is a discrete version of the objective function.

2.2 Mathematical and Numerical Issues

When the optimization problem is discretized with the finite element method, the zero lower bound on the design variables may cause the state matrix to become singular, and thus the state equation not uniquely solvable. To avoid this problem, the bounds are often changed into $\alpha(x) \in \{\varepsilon, 1\}$, where $\varepsilon > 0$, in the binary case, and to $\alpha(x) \in [\varepsilon, 1]$ in the relaxed case. The material indicator function α^*, corresponding to the computed optimal design for the relaxed problem, is in general not a binary function. One way of dealing with this problem, while remaining in a continuum for α, is to introduce a penalty that promotes values close to ε and 1. In topology optimization of linearly elastic structures, where the objective is to minimize the compliance of a structure with a constraint on the maximum weight of the structure, a common penalty strategy is to introduce an artificial density function such that elements with intermediate design values, that is $\varepsilon < \alpha < 1$, carry little stiffness compared to their weight [6, 51, 64]. Several artificial density functions are analyzed and compared by Bendsøe and Sigmund [8].

A more versatile approach to suppress intermediate values is to explicitly add a penalty function J_p to the objective function in problem (2.2). A commonly used penalty function, suggested for topology optimization by Allaire and Kohn [4], is

$$J_p = \gamma \int_\Omega (\alpha - \varepsilon)(1 - \alpha),$$

where γ is a constant representing the amount of penalization that should be used. The penalized problem may have many local minima, and the penalization also destroys any possible existence of solutions for the relaxed, nondiscretized problem. The ill-posedness of the binary problem causes the solutions of the discretized problem, whether binary or penalized, to depend on the size of the elements in the mesh. That is, the optimal design may radically change as the discretization is refined.

Below follows a short presentation of *restriction methods* used to treat the ill-posedness and the numerical instabilities that might occur. A systematic investigation of restriction methods with illustrative numerical examples for elastic continua is given by Borrvall [11]. Sigmund and Petersson [61] present an overview of numerical instabilities appearing in topology optimization.

The papers this thesis is based on use the filtering technique suggested by Bruns and Tortorelli [13]. This technique optimizes over an auxiliary function $\widetilde{\alpha}$ and lets the physical design α be defined through the convolution

$$\alpha(x) = \int_{\mathbb{R}^d} \Phi(x, y)\widetilde{\alpha}(y)\,\mathrm{d}y,$$

where the kernel Φ has compact support and d is the number of space dimensions. The measure of the kernel's support can be used as a tool specifying the minimal size of the parts in the design. Bourdin [12] studies a filtered version, with a fixed kernel, of the minimum compliance topology optimization problem, proves existence of solutions, and shows that one obtains convergence of solutions to the finite element discretized version of the problem. An alternative approach that solves the problems listed above is to add a constraint or a penalty on the perimeter or the gradient of the design [5, 31, 43, 48].

Another problem is that the numerically optimal design might have regions of checkerboard-like structures. This problem originates from at least one of: improper choice of finite elements in the discretization, or nonuniqueness of solutions (in the continuum problem) [47]. These problems are normally treated by choosing the proper elements or filtering [12, 13, 59].

2.3 Alternative Methods for Topology Optimization

Besides the material distribution method there exist several other techniques to solve topology optimization like problems as outlined above. The first methods for continuum structures were build around homogenization ideas (averaging heterogeneous media to derive effective properties) and employed composite materials to find optimal microstructures. The base of this approach is that it is often advantageous to have many tiny inclusions of one material in the other than just a few large ones. The recent books on structural optimization by Cherkaev [17] and Allaire [2] discuss homogenization principles in detail and present many applications.

The *bubble method* treats the topology optimization problem by solving a sequence of boundary shape optimization problems. The method generates several possible topologies, and a criterion for the maximum number of holes must follow external demands on the construction [25]. A related method is based on the level set method [44] for tracking the evolution of moving boundaries and topology changes in the optimization. In 1996 Santosa [54] described how this technique can be used to solve inverse problems and showed results reconstructing a diffraction screen. Here, the evolution was based on gradients of an objective function. Many contributions considering inverse scattering followed. A majority of these focused on the reconstruction of binary media using gradient-type evolution for the level set [3, 15, 24, 33, 40, 50, 58]. The versatility of the level set method is illustrated by its wide range of applications. A recent study by Burger & Osher [16] focuses on level set methods for inverse problems and optimal design. Dorn & Lesselier [23] review level set methods applied to inverse scattering problems.

An interesting (but computationally expensive) approach for the discrete problems, is to keep the condition that the design α is binary throughout the discretization. Stolpe and Svanberg [65] show that a large class of non-linear 0–1 topology optimization problems also can be modeled as linear mixed 0–1 problems. Svanberg and Werme utilize a hierarchical method with a neighborhood search to optimize discretized load-carrying structures [66, 67], and Stolpe [63] uses a branch-and-bound technique to find the global optimum of minimum weight truss problems.

3. Summary of Papers

3.1 Acoustic Wave Propagation Problems, Papers I–IV

3.1.1 Background

Acoustic devices operating as parts of a loudspeaker system have a large impact on the quality of the sound reproduction. Horns are used in such systems both to improve the efficiency and to direct sound toward the audience. The left illustration in Figure 3.1 depicts the setup used as basis for the optimization. The geometry is assumed to be infinite in the direction normal to the plane. The wave transducer consists of a waveguide with a funnel-shaped termination (the horn). A wave propagating through the waveguide can be expressed as a superposition of modal components. For the studied problem it is possible to choose the dimensions such that only the planar wave mode propagate in the waveguide. When a single frequency planar wave moving from left to right in the waveguide reaches the horn, parts of it will propagate out from the horn while other parts get reflected back into the waveguide. The transmission efficiency of the horn can be measured by comparing the amplitudes of the incoming right-going wave and the reflected left-going wave. The directivity describes the angular distribution of the radiated wave in the far field. When designing an acoustic horn, it is desired to have high transmission efficiency as well as control over the directivity of the horn.

3.1.2 Model

The walls of the waveguide and the horn consist of a sound-hard solid material and all other parts of space consist of air. The topology optimization

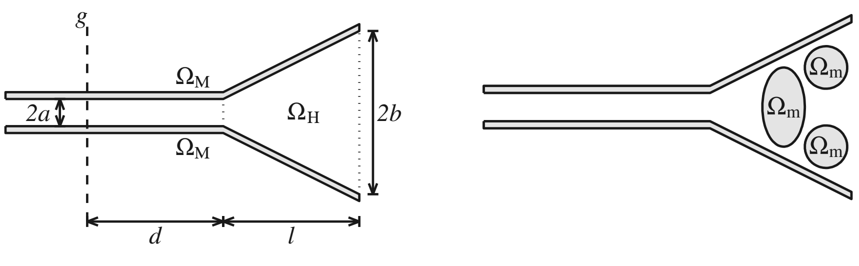

Figure 3.1: Material is placed in the region $\Omega_{\mathrm{m}} \subset \Omega_{\mathrm{H}}$ to improve the horn's radiation properties. The dotted lines in the left figure mark the left and right boundaries of the region Ω_{H} and are not part of the structure.

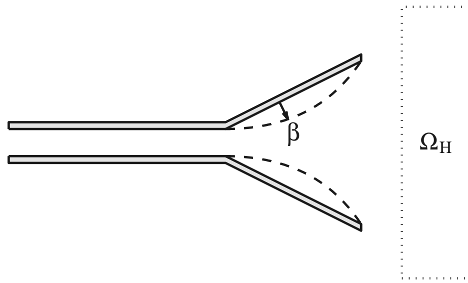

Figure 3.2: In Paper IV the walls of the horn are displaced and material is placed in the region Ω_H to improve the radiation properties.

problem in Papers I and II consists of finding the region $\Omega_m \subset \Omega_H$ where solid material is to be placed to get optimal performance of the horn. The design optimization problem in Paper IV consists of a horn whose flare is subject to boundary shape optimization together with an area Ω_H where solid material is placed using topology optimization techniques (Figure 3.2). The presence of material in the region is modeled by the material indicator function α (the characteristic function of the region Ω_m).

Assume that the wave propagation is governed by the wave equation for the acoustical pressure P',

$$\frac{\partial^2 P'}{\partial t^2} = c^2 \Delta P',$$

where c is the speed of sound. Seeking time harmonic solutions for a single frequency ω making use of the ansatz $P'(x,t) = \Re\{e^{i\omega t} p(x)\}$, where $\Re$ denotes the real part and i the imaginary unit, the above equation reduces to the following Helmholtz equation for the *complex amplitude function* p in the region of wave propagation,

$$c^2 \Delta p + \omega^2 p = 0. \tag{3.1}$$

Further, assuming that the horn is the only sound source, all waves are outgoing in the far field. This is equivalent to stipulating that p satisfies the Sommerfeld radiation condition

$$\lim_{|x|\to\infty} |x|^{(d-1)/2} \left(\frac{x}{|x|} \cdot \nabla p + ikp \right) = 0 \tag{3.2}$$

uniformly for all directions, where d is the number of space dimensions considered. In the far field, the complex amplitude function is essentially the product of a function of the distance to the origin and a function of the direction. More precisely, let $\rho > 0$, and let $\widehat{x}(\theta)$ be a point on the unit sphere, where θ represents the polar argument(s) of $\widehat{x}$. Then for $x_0 = \rho\widehat{x}$,

$$p(x_0) = \frac{e^{-ik\rho}}{\rho^{(d-1)/2}} \left\{ p_\infty(\theta) + O\left(\frac{1}{\rho}\right) \right\} \qquad \rho \to +\infty,$$

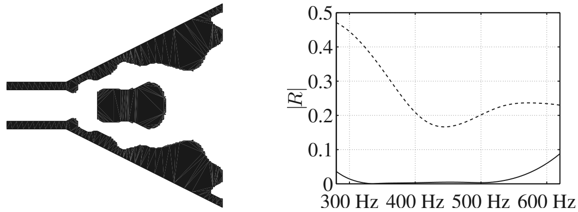

Figure 3.3: Horn from Paper I optimized for high efficiency at the frequencies 400 Hz, 410 Hz, …, 500 Hz and its reflection spectra (solid line). The dashed line illustrates the performance of the funnel shaped reference horn.

where $k = \omega/c$ is the wave number. The function $p_\infty(\theta)$ is denoted the *far-field pattern* of the horn. Paper III presents a derivation of the expression above for time harmonic acoustic wave propagation in two and three space dimensions, and includes detailed descriptions of the numerical evaluation of the far-field pattern in some typical situations. The presentation covers all parts required for computing the far-field properties of acoustical devices.

When optimizing the performance of the device in Papers I, II, and IV, problem (3.1) is solved using the finite element method on a bounded domain Ω. At the outer boundary of Ω the outgoing wave property is imposed artificially. This can be done by either imposing a radiation boundary condition at the boundary or by modifying the governing equation in a layer near this outer boundary.

3.1.3 Selected Results

The wave propagation in the waveguide at cross section g (Figure 3.1) consists essentially of one right-going (the incoming) and one left-going (the reflected) wave, with amplitudes A and B respectively. The reflection coefficient

$$R = \frac{|B|}{|A|}$$

depends on the frequency of the incoming wave as well as the shape of the horn. In Paper I, our objective is to maximize the efficiency, that is, to minimize the reflection coefficient of the horn. Figure 3.3 depicts a horn optimized for efficiency in the range 400–500 Hz and its reflection spectra. To attain this objective, the numerical algorithm minimizes the reflection coefficient at frequencies 400 Hz, 410 Hz, …, 500 Hz.

In Paper II, we include requirements on the efficiency as well as on the directivity of the horn. Figure 3.4 shows two optimal horns from Paper II. The left horn is optimized for maximum efficiency at 1200 Hz, and the right horn is optimized for maximum efficiency and at the same time minimal energy along the horn axis at 1200 Hz. Even though these requirements are in conflict, the algorithm finds a design with a good trade off between the two objectives with almost perfect transmission (zero reflection coefficient) and a

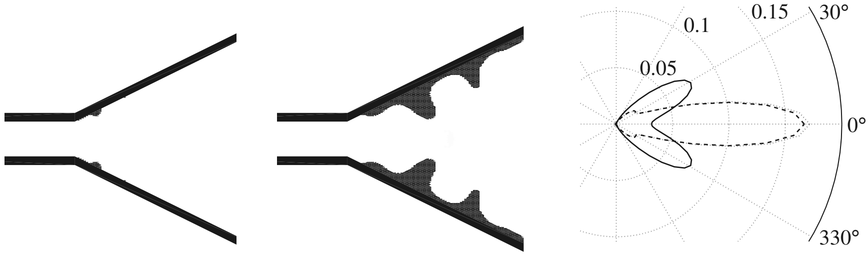

Figure 3.4: Optimization with respect to efficiency and far-field behavior for a single frequency of 1200 Hz. Left: horn optimized only with respect to efficiency. Middle: horn optimized with respect to both efficiency and far-field behavior. Right: far-field behavior for the funnel shaped reference horn (dashed line), the horn optimized with respect to efficiency (dotted line) and the horn optimized with respect to both efficiency and far-field behavior (solid line).

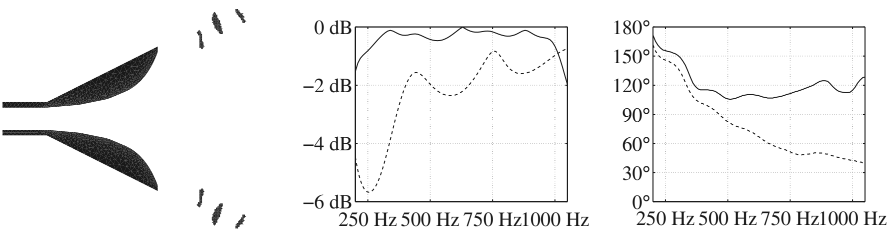

Figure 3.5: Horn with lens optimized for high efficiency and even directivity using modifications of the horn flare and topology optimization of the lens in front of the horn (left), the transmission loss in dB (middle), and the beamwidth (right) as functions of frequency. The solid lines in the diagrams correspond to the horn–lens combination, while the dashed line illustrates the performance of the funnel shaped reference horn without a lens.

low intensity along the horn axis. However, this design does not perform well at other frequencies as can be seen in Paper II.

It is difficult to obtain both high transmission efficiency as well as control over the far-field behavior using solely modifications in the horn region [68]. In Paper IV, we let material be arbitrarily placed in a region in front of the horn using topology optimization, while using boundary shape optimization of the horn flare to design a device with high efficiency and a wide beamwidth (angular distance between the −6 dB points in the far-field) for a wide range of frequencies. Aiming at creating an efficient device with beamwidth above 100° in the frequency range 250–1000 Hz, this approach produces the horn–lens combination in Figure 3.5. The solid line in the diagrams illustrate the behavior of the optimized horn–lens combination while the dashed line corresponds to the funnel shaped reference horn. Compared with the reference horn, the optimized horn–lens combination is more efficient and has a superior beamwidth throughout the frequency band of interest.

3.2 Microwave Tomography, Papers V–VII

3.2.1 Background

In tomography, images depicting cross sections of objects are created. Medical tomographic systems are based on identification of tissue properties. Microwave tomography is a technique in which microwaves illuminate a specimen, and measurements of the scattered electrical field are used to determine and depict the specimen's dielectric and conductive properties. Important physiological conditions of living tissues, such as blood flow reduction and the presence of malignancy, are accompanied with changes in dielectric properties [37, 56, 57]. Due to the low energy of photons in the microwave region, the radiation is not ionizing, in contrast to x-rays. Hence, microwave tomography is expected to be safer than x-ray based tomography. However, the desired resolution in microwave tomography is of the same size or smaller than the used wavelengths. Thus, the fast ray-theory based algorithms [38] for x-ray and ultrasound tomography cannot be expected to give satisfactory results.

A mathematical model for microwave tomography is to fit a complex permittivity function in the Maxwell equations for a given set of measurements. The first algorithms for microwave tomography focused on the low contrast case, that is, the reconstruction of objects with only small spatial variations in the permittivity. Kak and Slaney [38] review these so called fast diffraction tomography methods as well as classical ray theory based methods. However, biological tissues show high contrasts in permittivity, for instance due to differences in water content. Therefore, medical applications necessitate methods that can handle the high-contrast case. The most straightforward—and computationally expensive—way to eliminate the contrast restrictions is simply to attack the original nonlinear least-squares problem with a numerical method [1, 14, 27, 28, 36, 41, 55, 56, 62]. To decrease the computational cost, most authors assume symmetries so that the governing Maxwell equations reduce to the scalar Helmholtz equation. Papers V–VII address the problem of reconstructing the dielectric properties of biological objects using topology optimization methodologies under the above mentioned symmetry assumptions.

3.2.2 Modeling

The problem consists of reconstructing the dielectric properties of unknown objects located inside a hexagonal metallic container with side length 16 cm. The objects are located in the region $\Omega_?$ (Figure 3.6) and embedded in a saline solution with known dielectric properties, ε_s. A 2.2 cm wide waveguide filled with a low loss-material with known dielectric properties ε_wg is attached to each side of the container. At the end of each waveguide there is a device able to radiate microwaves as well as measure the electric field. The setup as well as the unknown objects are assumed to extend infinitely in the direction normal to the plane.

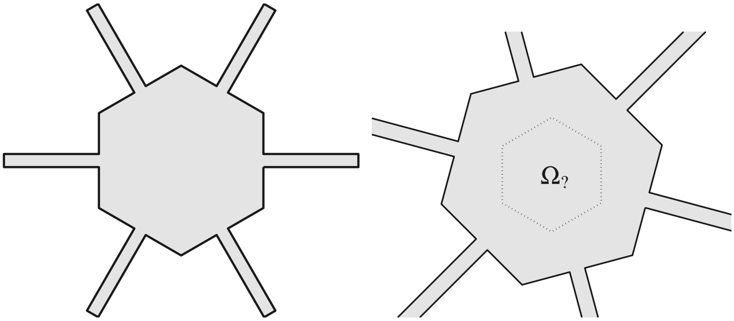

Figure 3.6: The problem consists of finding the dielectric properties of unknown objects. Left: a set of microwave transmitters and receivers are located at the ends of the waveguides. Right: the container can be rotated with respect to the region $\Omega_?$, in which the unknown objects are located.

The Maxwell equations govern the electrical field vector E, which is assumed to be polarized normal to the plane. Under the above polarization assumptions, it is equivalent to consider the setup to extend only a finite length normal to the plane, and being terminated by plates of perfectly conducting material.

Figure 3.6 illustrates the computational domain Ω. The sides of the container and the waveguides consist of perfectly conducting material. The outer ends of the waveguides are denoted $\Gamma_{\text{in}}^{(n)}$, $n = 1, 2, \ldots, 6$ and their union Γ_{in}. The devices at the end of the waveguides are simulated with a Somerfeld approximation prescribing an incoming lowest mode wave while assuring that all outgoing modes are absorbed. Letting $\mathcal{V} = \{v \in H^1(\Omega) \mid v = 0 \text{ on } \partial\Omega - \Gamma_{\text{in}}\}$ and seeking time harmonic solutions for the wave propagation problem with source located at waveguide m, angular frequency ω, using the ansatz $E(x,t) = \mathbb{R}\{(0,0,u)\mathrm{e}^{\mathrm{i}\omega t}\}$ result in that the complex amplitude function u satisfies the variational form: Find $u \in \mathcal{V}$ such that

$$\int_\Omega \nabla u \cdot \nabla v - k_0 \int_\Omega \varepsilon u v + \mathrm{i}\widehat{k} \int_{\Gamma_{\text{in}}} u v = 2\mathrm{i}\widehat{k} A \int_{\Gamma_{\text{in}}^{(m)}} \cos\left(\frac{(x - x_m) \cdot t_m \pi}{d}\right) v, \quad (3.3)$$

for all $v \in \mathcal{V}$. All components of the variational form above are detailed in Papers V–VII.

3.2.3 Optimization problem

To depict the unknown dielectric properties, the electric field is observed at a number of different illumination conditions. To achieve a good reconstruction, multiple frequencies are used; moreover, the container can be rotated (as illustrated to the right in Figure 3.6) at angles $\theta_l \in [0°, 60°)$, $l = 1, 2, \ldots, L$ with respect to $\Omega_?$. For each rotation angle θ_l and frequency ω_k, the devices at the ends of the waveguides one at a time radiate the objects, and the resulting electrical field is measured by all six devices.

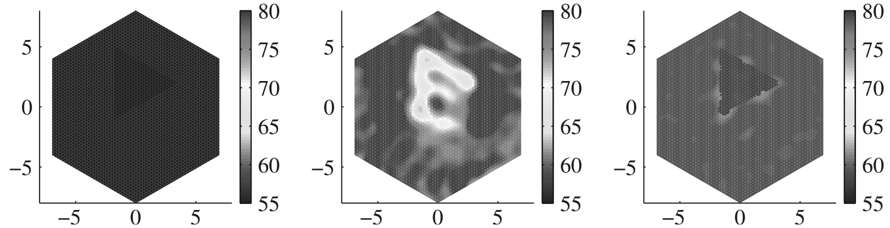

Figure 3.7: Real part of selected permittivity distributions from Paper V. Reconstructing the phantom (left) using 144 observations and no a priori information (middle) as well as a priori information that the dielectric properties are either $\varepsilon_1 = 79.0 - 10.5\mathrm{i}$ or $\varepsilon_2 = 57.5 - 22.6\mathrm{i}$ inside $\Omega_?$ (right). The scales on the axes are in centimeters.

For source location $\Gamma_{\mathrm{in}}^{(n)}$, rotation angle θ_l, and frequency ω_k, let $v_{n,m}^{k,l}$ denote the target (or measured) mean complex value over $\Gamma_{\mathrm{in}}^{(m)}$. The problem of finding the dielectric properties is mathematically formulated as the following nonlinear least squares problem:

$$\min_{\varepsilon} \sum_{k,l} \sum_{m,n=1}^{6} \left| \langle u(\varepsilon)_n^{k,l} \rangle_m - v_{n,m}^{k,l} \right|^2, \tag{3.4}$$

where $\langle u(\varepsilon)_n^{k,l} \rangle_m$ denote the average over $\Gamma_{\mathrm{in}}^{(m)}$ of the solution $u_n^{k,l}$ to (3.3) with source located at $\Gamma_{\mathrm{in}}^{(n)}$, at rotation angle θ_l, and frequency ω_k.

3.2.4 Selected Results

In Paper V we prove that problem (3.4) has at least one solution for any set of complex measurements. We first show that for each permittivity distribution, there exists a unique solution to the forward problem (3.3). To prove the existence of a solution to problem (3.4) we utilize properties concerning compact inclusion of Sobolev spaces and a trace theorem for domains with Lipschitz boundaries.

The numerical experiments in Paper V aim to find a triangular phantom, with permittivity $\varepsilon = 57.5 - 22.6\mathrm{i}$ using incoming waves with frequency 900 MHz. At this frequency, the dielectric properties of the phantom correspond to those of soft tissue. Figure 3.7 shows the real part of the phantom (left) and two reconstructed versions of this phantom (middle and right image). The left image also illustrates the mesh, which has 6144 elements in the region $\Omega_?$ where the unknown objects are located. The middle image was reconstructed using 24 irradiation positions, resulting in a total of 144 observations. By making use of these observations the 6144 unknowns are reconstructed in (only!) 12 iterations of the optimization algorithm. As opposed to topology optimization for structures, there is no indication of mesh dependency and checkerboarding when forcing the permittivity to attain discrete values. Using that the dielectric properties are either

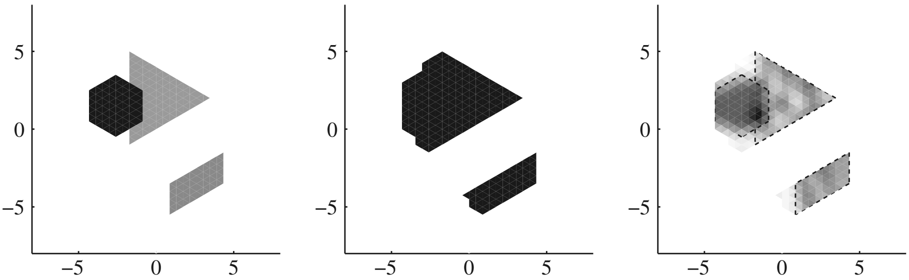

Figure 3.8: Sum of real and imaginary part of selected permittivity distributions from Paper VI. Reconstructing the phantom (left) using a priori information that all elements not marked black in the middle image contain saline solution. The image on the right shows the reconstructed properties. The scales on the axes are in centimeters.

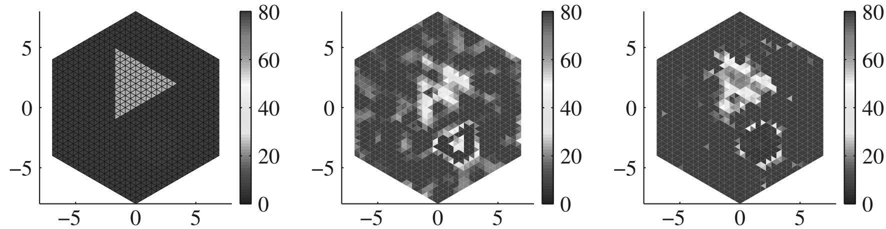

Figure 3.9: Real part of selected permittivity distributions from Paper VII. Reconstructing the phantom (left) by solving a sequence of topology optimization problems. A priori information about the permittivities and the solution of the current problem defines the next problem in this sequence. The middle image shows the permittivity distribution after the first problem and the right image shows the permittivity distribution after five problems. The scales on the axes are in centimeters.

$\varepsilon_1 = 79.0 - 10.5\mathrm{i}$ or $\varepsilon_2 = 57.5 - 22.6\mathrm{i}$ inside $\Omega_?$ and 24 irradiation positions we obtain an almost perfect reconstruction of the permittivity; the right of Figure 3.7 depicts the real part of this reconstructed permittivity distribution.

In Paper VI we use frequencies in the range 870–930 MHz to reconstruct the dielectric properties of three phantoms. The images in Figure 3.8 show the sum of the real and imaginary part of the dielectric properties. The left image illustrates one of the phantoms. The triangular specimen has dielectric properties corresponding to muscle, the hexagonal specimen correspond to fat, and the parallelogram shaped object corresponds to blood. In many real life applications, some geometric properties of the unknown objects are known or can easily be obtained, for example through laser measurements. Here, the reconstruction of the dielectric properties uses that all elements not marked black in the middle image of Figure 3.8 contain the saline solution; the four frequencies 870, 890, 910, and 930 MHz; and 24 irradiation positions per frequency. The right image in Figure 3.8 depicts the dielectric properties reconstructed using this approach and simulated numerical data with an approximate signal-to-noise ratio of 40 dB.

Paper VII presents a subdomain identification strategy that uses information about the permittivities of unknown objects to construct successively a sequence of problems. Each problem in this sequence is constructed using the solution of the previous one in combination with available a priori information about the distribution of the unknown permittivities in the complex plane. Figure 3.9 illustrates the benefits of using this approach. The left image depicts the real part of the phantom; the mesh in the background has 1536 elements in $\Omega_?$ and is used in the reconstruction. The image in the middle is reconstructed using the three frequencies 875, 900, and 925 MHz. The image on the right is reconstructed using the same data, but with applying the subdomain identification strategy and a sequence of five problems.

3.3 Large Scale Topology Optimization Using a GPU, Paper VIII

3.3.1 Background

Material distribution problems are typically cast as nonlinear programming problems over the coefficients in a partial differential equation. To avoid a priori bias, the coefficient field is represented as large (for high resolution) arrays of equally-sized elements (pixels). Such large scale pixel based topology optimization problems demand much computational power and time. An important step toward solving complicated large scale problems is the development of efficient and parallel algorithms and implementations tailored for these problems.

During the last years, the computational power of graphics processing units (GPUs) has increased at a much higher rate than the corresponding rate for regular CPUs. Compared to a typical CPU, the GPU allocates more transistors to data processing and less to caching and flow control. As a consequence, the hardware architecture imposes an algorithmic constraint on the class of problems that benefit from GPU acceleration. Candidate problems need to be solvable by algorithms for which data-parallel computations dominate the computational effort. One example of such problems is, as shown in Paper VIII, large scale pixel based topology optimization problems. This contribution is in line with a current trend to utilize the highly parallel architecture of the GPU to accelerate the solution of various problems [22, 32, 45, 53].

3.3.2 Model Problem

The model problem studied in Paper VIII consists of a rectangular plate subject to constant heating. The plate occupies the unit-size two dimensional domain Ω (Figure 3.10) whose boundary consists of parts Γ_D and Γ_N. The plate is insulated along Γ_N and held at constant temperature at Γ_D. Now assume that we have a limited amount of a high conductivity material ($\kappa = \overline{\kappa}$) and an unlimited amount of a low conductivity material ($\kappa = \underline{\kappa}$). We seek to distribute

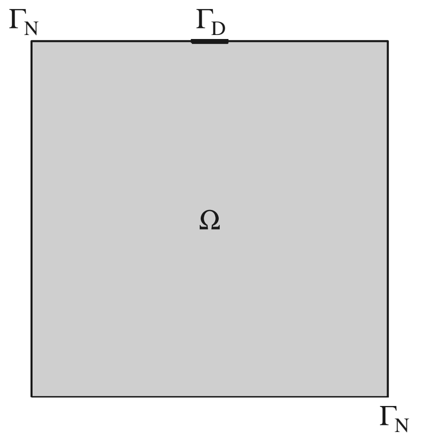

Figure 3.10: The problems consist of finding the distribution within Ω of two materials with different heat conduction properties in order to obtain a temperature distribution that is as even as possible.

these two materials in order to obtain a temperature field that is as "even" as possible at thermal equilibrium and formulate our material distribution problem as

$$\begin{aligned}
\min_{\alpha \in \mathcal{U}} \quad & \int_\Omega Tf \\
\text{subject to} \quad & -\nabla \cdot (\kappa \nabla T) = f \text{ in } \Omega, \\
& T = 0 \text{ on } \Gamma_D, \\
& (\kappa \nabla T) \cdot n = 0 \text{ on } \Gamma_N, \\
& \kappa = \underline{\kappa} + \alpha(\overline{\kappa} - \underline{\kappa}), \\
& \int_\Omega \alpha \leq V,
\end{aligned} \tag{3.5}$$

where T is the temperature, f the constant heat source density, n the unit normal on Γ_N, α our design variable,

$$\mathcal{U} = \{\alpha \in L^\infty(\Omega) \mid \alpha(x) \in \{0, 1\} \text{ a.e. in } \Omega\},$$

and V corresponds to the available amount of the high conductivity material.

3.3.3 Selected Results

To solve the material distribution problem efficiently, we relax the binary constraint on α using the SIMP (Solid Isotropic Material with Penalization) approach [6]. We partition the domain into $N = n^2$ squares (elements) and use filtering with support within a fixed number of elements. This filter stabilizes the numerical procedure without imposing a smallest geometry scale. We discretize the governing equation for the temperature field using the finite ele-

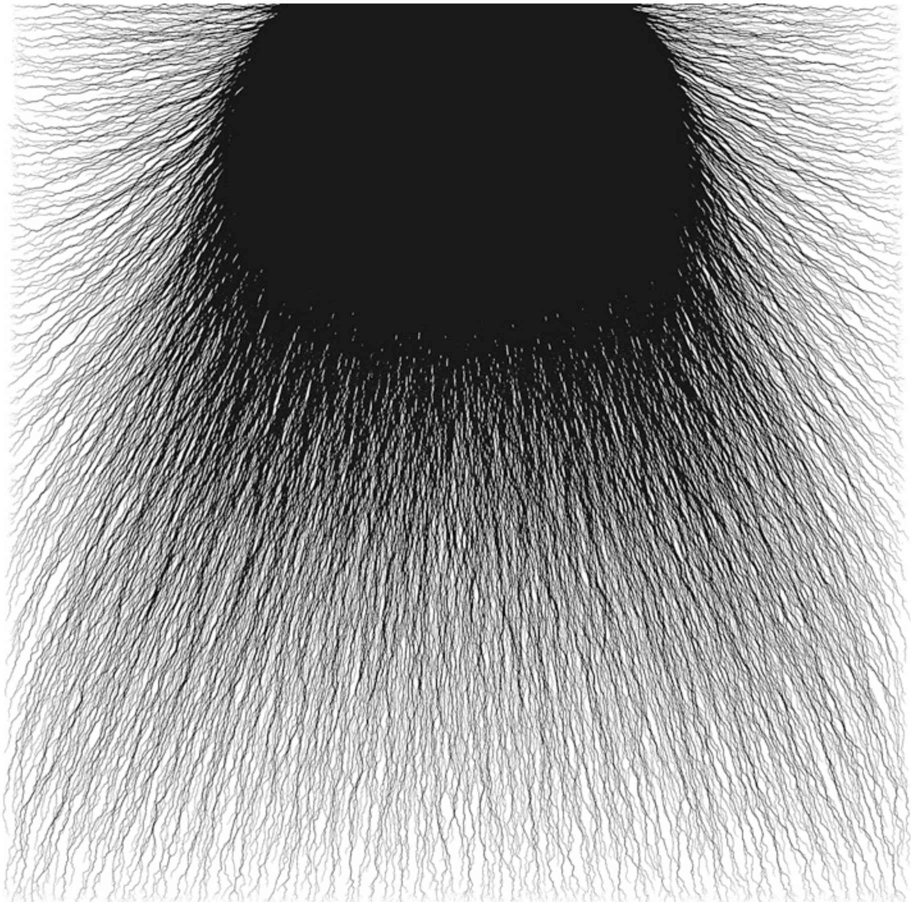

Figure 3.11: Material distribution optimized using $N = 2100^2$ elements allowing high conductivity material (black) to fill a relative volume fraction $V = 0.5$ of the plate.

ment method with bilinear elements. The preconditioned conjugate gradient method solves the resulting linear system. We solve a discrete version of problem (3.5) numerically on the GPU with the gradient based optimality criteria method (see for example § 1.2 in Bendsøe and Sigmund's book [9] for a more detailed description). Figure 3.11 shows the resulting material distribution for $N = 2100^2$ and $V = 0.5$. In this case, the nonlinear optimization problem has over 4 million design variables.

To compare the running time for the algorithm on the GPU with typical CPU-based implementations, we implement a serial version of the algorithm as well as an OpenMP parallelized version. We run the GPU and the single core CPU versions of the algorithm on a workstation equipped with an 1.86 GHz Intel Core 2 Duo processor and a NVIDIA 8800 GTX based graphics card. The parallel version of the algorithm is executed on an AMD Opteron 2220 (2.80 GHz) based HPC machine. Figure 3.12 shows the time per iteration for the three experimental setups described above. For the larger prob-

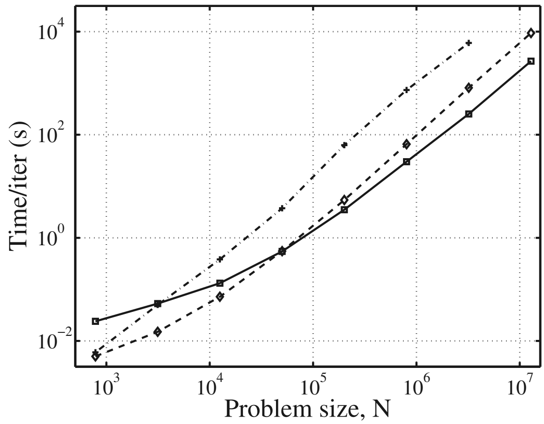

Figure 3.12: Iteration time in seconds as a function of problem size for the different experimental setups. The solid line illustrates the computational time on the GPU. The dash–dotted line presents the computational time on a single core on the 1.86 GHz Intel Core 2 Duo processor. The dashed line shows the computational time on four cores on a 2.80 GHz AMD Opteron 2220 based HPC cluster.

lems, the GPU based version is about 20 times faster than the single core CPU version and about three times faster than the parallelized version running on the HPC machine.

4. Sammanfattning på svenska

I alla tider har människan utfört undersökningar och experiment för att förstå hur saker och ting fungerar. Alla är inte lika intresserade av att experimentera och undersöka olika system. Däremot är det i allmänhetens intresse att det framställs nya alster och utformningar som fungerar bättre än föregångarna. Drömmen för varje formgivare är skapa ett optimalt system eller formge den ultimata produkten. För att uppfylla denna dröm måste man först definiera vad som menas med att någonting är optimalt. Exempelvis kan optimalitet avse att systemet har minimal energiförlust, största förväntade vinst, är mest estetiskt tilltalande eller någonting annat som formgivaren bestämmer sig för. Denna avhandling behandlar problem där prestanda kan mätas. Det finns alltså en *målfunktion* som för en given utformning producerar ett tal som beskriver dess prestanda. En utformning sägs vara optimal om värdet på målfunktionen är så lågt eller högt (beroende på vilket mål som eftersträvas) som möjligt. Vidare antas det att den bakomliggande fysiken kan beskrivas matematiskt via en *tillståndsekvation*.

Inom industrin krävs det oftast att utformningen håller sig inom ett visst begränsat utrymme, *designområdet*, det är också vanligt att det finns ytterligare *bivillkor* som begränsar formgivarens valmöjligheter. Exempelvis, när man ska bygga en bro så vill man att byggkostnaden ska vara så låg som möjligt (mål eller objekt), men man kräver även att bron kan bära minst en viss förutbestämd belastning (bivillkor). Vanligtvis är utformningsprocesser iterativa. Först föreslås och provas en utformning. När detta är gjort görs förändringar och finjusteringar varefter den nya utformningen testas. Denna process repeteras tills inga ytterligare förbättringar är möjliga.

I takt med att datorer har blivit kraftfullare har datorsimuleringar blivit kostnads- och tidseffektiva komplement till traditionella experiment. Under designprocessen används ofta datorsimuleringar för att evaluera prestandan hos en given konfiguration. Ett alternativ till manuell finjustering av utformningen och en utmärkt användning av datorers beräkningskraft är att använda sig av numerisk formoptimering. Vid dessa simuleringar parameteriseras geometrin varpå parameterrymden genomsöks för att finna den optimala utformningen. Detta görs genom att algoritmen systematiskt evaluerar prestandan (målfunktionen) för olika parameterkombinationer. Parameteriseringen av geometrin utgår ofta från en given referenskonfiguration. Valet av parameterisering spelar en avgörande roll för slutresultaten. Datorprogrammet kan trots allt inte göra mer än att söka igenom hela den givna parameterrymden och således kan den resulterade optimala utformningen variera när parameteriseringen ändras.

Numerisk formoptimering kan delas upp i tre huvudgrenar: *storleksoptimering*, *randformoptimering* och *topologioptimering*. Storleksoptimering består av problem där formen, men ej storleken av alla delar i en konstruktion, redan är given. Det som söks i dessa problem är alltså de optimala storlekarna för delarna. I randformoptimering studeras problem där formen av objektet inte är föreskriven. I dessa problem undersöks geometriförändringar givna via randförskjutningar, vilket är en utmärkt strategi för att göra de sista finjusteringarna av en utformning. Topologioptimering behandlar problem där man från början inte gör några antaganden beträffande utforming. I dessa problem får utformningen växa fram och hål respektive fritt svävande delar kan uppkomma eller försvinna under processen.

Topologioptimering för kontinuumstrukturer är ett relativt ungt forskningsområde som har utvecklats snabbt under det senaste två årtiondena. Topologioptimering för strukturmekanik är idag ett moget område och används för att framställa och förbättra nya produkter inom exempelvis bil- och flygindustrin. Under det senaste årtiondet har forskare börjat applicera liknande strategier på problem inom andra discipliner, såsom vågutbrednings- och strömningsproblem. Min forskning fokuserar på användandet av topologioptimering för vågutbredningproblem. Mitt mål är att göra dessa strategier lika framgångsrika för vågutbredning som de är för strukturmekaniska problem. Denna avhandling behandlar topologioptimering för vågproblem och är baserad på åtta artiklar vars innehåll beskrivs kort nedan.

Artikel I–IV fokuserar på akustisk vågutbredning och utformningen av akustiska horn. En viktig egenskap hos ett akustiskt horn är dess effektivitet. Artikel I använder topologioptimering för att utforma horn med hög effektivitet. En annan viktig aspekt är hornets fjärrfältsegenskaper (den akustiska energins riktningskarakteristik vid stora avstånd). Artikel II visar horn optimerade med avseende på både effektivitet och fjärrfältsegenskaper. Den numeriska behandlingen av fjärrfältsegenskaperna redogör Artikel III för. För att att uppnå en jämn spridning och hög effektivitet använder sig Artikel IV av randformsoptimering för hornet och låter topologioptimeringsstrategier placera en lins framför hornet så att önskade fjärrfältsegenskaper uppnås.

Medicinsk tomografi används för att framställa bilder av tvärsnitt av biologiska objekt. I mikrovågstomografi avbildas vävnadernas dielektiska egenskaper. Många fysiologiska förändringar, exempelvis minskat blodflöde och maligna vävnader medför signifikanta ändringar i de dielektriska egenskaperna, vilket gör att dessa kan upptäckas med mikrovågstomografi utan speciella kontrastvätskor. Vidare är mikrovågor ickejoniserande och förväntas vara säkrare och billigare än röntgen. Däremot gör de långa våglängderna att rekonstruktionsproblemet blir mycket komplicerat. Artikel V–VII redogör hur rekonstruktionen av de dielektriska egenskaperna kan utföras med hjälp av topologioptimeringstekniker.

Slutligen beskriver Artikel VIII hur beräkningskraften hos en modern grafikprocessor kan användas för att lösa storskaliga topologioptimeringsproblem.

5. Acknowledgements

I am grateful to my advisor Martin Berggren who introduced me to this interesting subject. Martin, you have been an excellent guide through all phases of my work on this thesis. I thank all my colleagues for making this work easier and even more enjoyable. I am glad that my family and friends always encourage me and give me endless support. Thank you everybody! I hope that I will get the opportunity to meet you often in the future. Finally, I thank the Swedish Research Council (Vetenskapsrådet) for financially supporting this work.

References

[1] A. Abubakar, P. M. van den Berg, and J. J. Mallorqui. Imaging of biomedical data using a multiplicative regularized contrast source inversion method. *IEEE Transactions on Microwave Theory and Techniques*, 50(7):1761–1771, 2002. doi:10.1109/TMTT.2002.800427.

[2] G. Allaire. *Shape Optimization by the Homogenization Method*. Applied Mathematical Sciences. Springer, 2002.

[3] G. Allaire, F. Jouve, and A.-M. Toader. Structural optimization using sensitivity analysis and a level-set method. *Journal of Computational Physics*, 194(1):363–393, 2004. doi:10.1016/j.jcp.2003.09.032.

[4] G. Allaire and R. V. Kohn. Topology optimization and optimal shape design using homogenization. In M. P. Bendsøe and C. A. Mota Soares, editors, *Topology design of structures*, pages 207–218. Kluwer Academic Publisher, 1993.

[5] L. Ambrosio and G. Buttazzo. An optimal design problem with perimeter penalization. *Calculus of Variations and Partial Differential Equation*, 1(1):55–69, 1993. doi:10.1007/BF02163264.

[6] M. P. Bendsøe. Optimal shape design as a material distribution problem. *Structural Optimization*, 1:193–202, 1989. doi:10.1007/BF01650949.

[7] M. P. Bendsøe and N. Kikuchi. Generating optimal topologies in structural design using a homogenization method. *Computer Methods in Applied Mechanics and Engineering*, 71:197–224, 1988. doi:10.1016/0045-7825(88)90086-2.

[8] M. P. Bendsøe and O. Sigmund. Material interpolation schemes in topology optimization. *Archive of Applied Mechanics*, 69:635–654, 1999. doi:10.1007/s004190050248.

[9] M. P. Bendsøe and O. Sigmund. *Topology Optimization. Theory, Methods, and Applications*. Springer, 2003.

[10] P. Borel, A. Harpøth, L. Frandsen, M. Kristensen, P. Shi, J. S. Jensen, and O. Sigmund. Topology optimization and fabrication of photonic crystal structures. *Optics Express*, 12(9):1996–2001, 2004.

[11] T. Borrvall. Topology optimization of elastic continua using restriction. *Archives of Computational Methods in Engineering*, 8(4):351–385, 2001.

[12] B. Bourdin. Filters in topology optimization. *International Journal for Numerical Methods in Engineering*, 50:2143–2158, 2001. doi:10.1002/nme.116.

[13] T. E. Bruns and D. A. Tortorelli. Topology optimization of non-linear elastic structures and compliant mechanisms. *Computer Methods in Applied Mechanics and Engineering*, 190:3443–3459, 2001. doi:10.1016/S0045-7825(00)00278-4.

[14] A. E. Bulyshev, A. E. Souvorov, S. Y. Semenov, V. G. Posukh, and Y. E. Sizov. Three-dimensional vector microwave tomography: theory and computational experiments. *Inverse Problems*, 20(4):1239–1259, 2004. doi:10.1088/0266-5611/20/4/013.

[15] M. Burger. A level set method for inverse problems. *Inverse Problems*, 17(5):1327–1355, 2001. doi:10.1088/0266-5611/17/5/307.

[16] M. Burger and S. J. Osher. A survey on level set methods for inverse problems and optimal design. *European Journal of Applied Mathematics*, 16(2):263–301, 2005. doi:10.1017/S0956792505006182.

[17] A. Cherkaev. *Variational Methods for Structural Optimization*. Applied Mathematical Sciences. Springer, 2000.

[18] S. J. Cox and D. C. Dobson. Band structure optimization of two-dimensional photonic crystals in H-polarization. *Journal of Computational Physics*, 158(2):214–224, 2000. doi:10.1006/jcph.1999.6415.

[19] K. Culmann. *Die Graphische Statik*. Mayer und Zeller, Zürich, 1866.

[20] D. C. Dobson. Optimal mode coupling in simple planar waveguides. In M. P. Bendsøe, N. Olhoff, and O. Sigmund, editors, *IUTAM Symposium on Topological Design Optimization of Structures, Machines and Materials*, pages 301–310. Springer, 2006.

[21] D. C. Dobson and S. J. Cox. Maximizing band gaps in two-dimensional photonic crystals. *SIAM Journal on Applied Mathematics*, 59(6):2108–2120, 1999. doi:10.1137/S0036139998338455.

[22] T. Dokken, T. R. Hagen, and J. M. Hjelmervi. The GPU as a high performance computational resource. In B. Jüttler, editor, *Proceedings of the 21st spring conference on Computer graphics, Budmerice, Slovakia*, pages 21–26, New York, 2005. ACM Press.

[23] O. Dorn and D. Lesselier. Level set methods for inverse scattering. *Inverse Problems*, 22(4):R67–R131, 2006. doi:10.1088/0266-5611/22/4/R01.

[24] O. Dorn, E. L. Miller, and C. M. Rappaport. A shape reconstruction method for electromagnetic tomography using adjoint fields and level sets. *Inverse Problems*, 16(5):1119–1156, 2001. doi:10.1088/0266-5611/16/5/303.

[25] H. A. Eschenauer, V. V. Kobelev, and A. Schumacher. Bubble method for topology and shape optimization of structures. *Structural and Multidisciplinary Optimization*, 8(1):42–51, 1994. doi:10.1007/BF01742933.

[26] H. A. Eschenauer and N. Olhoff. Topology optimization of continuum structures: A review. *Applied Mechanics Reviews*, 54(4):331–390, 2001. doi:10.1115/1.1388075.

[27] Q. Fang, P. M. Meaney, and K. D. Paulsen. Microwave image reconstruction of tissue property dispersion characteristics utilizing multiple-frequency information. *IEEE Transactions on Microwave Theory and Techniques*, 52(8):1866–1875, 2004. doi:10.1109/TMTT.2004.832014.

[28] A. Fhager, P. Hashemzadeh, and M. Persson. Reconstruction quality and spectral content of an electromagnetic time-domain inversion algorithm. *IEEE Transactions on Biomedical Engineering*, 53(8):1594–1604, 2006. doi:10.1109/TBME.2006.878079.

[29] R. Glowinski. *Numerical simulation for some applied problems originating from continuum mechanics*, volume 195 of *Lecture Notes in Physics*, pages 96–145. Springer, Berlin / Heidelberg, trends and applications of pure mathematics to mechanics edition, 1984.

[30] J. Goodman, R. V. Kohn, and L. Reyna. Numerical study of a relaxed variational problem from optimal design. *Computer Methods in Applied Mechanics and Engineering*, 57(1):107–127, 1986. doi:10.1016/0045-7825(86)90073-3.

[31] R. B. Haber, C. S. Jog, and M. P. Bendsøe. A new approach to variable-topology shape design using a constraint on perimeter. *Structural Optimization*, 11(1–2):1–12, 1996. doi:10.1007/BF01279647.

[32] M. Harris, G. Coombe, T. Scheuermann, and A. Lastra. Physically-based visual simulation on graphics hardware. In *HWWS '02: Proceedings of the ACM SIGGRAPH/EUROGRAPHICS conference on Graphics hardware*, pages 109–118, Aire-la-Ville, Switzerland, 2002. Eurographics Association.

[33] K. Ito, K. Kunisch, and Z. Li. Level-set function approach to an inverse interface problem. *Inverse Problems*, 17(5):1225–1242, 2001. doi:10.1088/0266-5611/17/5/301.

[34] J. S. Jensen and O. Sigmund. Systematic design of photonic crystal structures using topology optimization: Low-loss waveguide bends. *Applied Physics Letter*, 84(12):2022–2024, 2004. doi:10.1063/1.1688450.

[35] J. S. Jensen and O. Sigmund. Systematic design of acoustic devices by topology optimization. In *Twelfth international congress on sound and vibration, ICVS12 2005, Lisbon*, 2005.

[36] N. Joachimowicz, C. Pichota, and J. P. Hugonin. Inverse scattering: an iterative numerical method for electromagnetic imaging. *IEEE Transactions on Antennas and Propagation*, 39(12):1742–1753, 1991. doi:10.1109/8.121595.

[37] W. T. Joines, Y. Zhang, C. Li, and R. L. Jirtle. The measured electrical properties of normal and malignant human tissues from 50 to 900 MHz. *Medical Physics*, 21(4):547–550, 1994. doi:10.1118/1.597312.

[38] A. C. Kak and M. Slaney. *Principles of Computerized Tomographic Imaging*. SIAM, Philadelphia, 2001.

[39] J. L. Lions. *Optimal control of systems governed by partial differential equations*, volume 170 of *Die Grundlehren der mathematischen Wissenschaften*. Springer, Berlin, 1971. Translated by S. K. Mitter.

[40] A. Litman, D. Lesselier, and F. Santosa. Reconstruction of a two-dimensional binary obstacle by controlled evolution of a level-set. *Inverse Problems*, 14(3):685–706, 1998. doi:10.1088/0266-5611/14/3/018.

[41] P. M. Meaney, K. D. Paulsen, A. Hartov, and R. K. Crane. Microwave imaging for tissue assessment: Initial evaluation in multitarget tissue-equivalent phantoms. *IEEE Transactions on Biomedical Engineering*, 43(9):878–890, 1996. doi:10.1109/10.532122.

[42] A. G. M. Michell. The limits of economy of material in frame-structures. *Philosophical Magazine Ser. 6*, 8(47):589–597, 1904.

[43] F. Niordson. Optimal design of elastic plates with a constraint on the slope of the thickness function. *International Journal of Solids and Structures*, 19(2):141–151, 1983. doi:10.1016/0020-7683(83)90005-7.

[44] S. Osher and J. A. Sethian. Fronts propagating with curvature-dependent speed: Algorithms based on Hamilton–Jacobi formulations. *Journal of Computational Physics*, 79(1):12–49, 1988. doi:10.1016/0021-9991(88)90002-2.

[45] J. D. Owens, D. Luebke, N. Govindaraju, M. Harris, J. Krüger, A. E. Lefohn, and T. J. Purcell. A survey of general-purpose computation on graphics hardware. *Computer Graphics Forum*, 26(1):80–113, 2007. doi:10.1111/j.1467-8659.2007.01012.x.

[46] C. H. Papadimitriou and K. Steiglitz. *Combinatorial Optimization, Algorithms and Complexity*. Dover, 1998.

[47] J. Petersson. A finite element analysis of optimal variable thickness sheets. *SIAM Journal on Numerical Analysis*, 36(6):1759–1778, 1999. doi:10.1137/S0036142996313968.

[48] J. Petersson. Some convergence results in perimeter-controlled topology optimization. *Computer Methods in Applied Mechanics and Engineering*, 171(1–2):123–140, 1999. doi:10.1016/S0045-7825(98)00248-5.

[49] L. S. Pontryagin, V. G. Boltyanskii, R. V. Gamkrelidze, and E. F. Mishchenko. *The mathematical theory of optimal processes*. Interscience, New York, 1962. Editor L. W. Neustadt, translated by K. N. Trirogoff.

[50] C. Ramananjaona, M. Lambert, D. Lesselier, and J.-.P Zolésio. Shape reconstruction of buried obstacles by controlled evolution of a level set: from a min-max formulation to numerical experimentation. *Inverse Problems*, 17(4):1087–1111, 2001. doi:10.1088/0266-5611/17/4/335.

[51] A. Rietz. Sufficiency of a finite exponent in SIMP (power law) methods. *Structural and Multidisciplinary Optimization*, 21:159–163, 2001. doi:10.1007/s001580050180.

[52] G. I. N. Rozvany. Aims, scope, methods, history and unified terminology of computer-aided topology optimization in structural mechanics. *Structural and Multidisciplinary Optimization*, 21(2):90–108, 2001. doi:10.1007/s001580050174.

[53] M. Rumpf and R. Strzodka. Level set segmentation in graphics hardware. In *International Conference on Image Processing, (ICIP'01)*, volume 3, pages 1103–1106, 2001.

[54] F. Santosa. A level-set approach for inverse problems involving obstacles. *ESAIM. Control, Optimisation and Calculus of Variations*, 1:17–33, 1996. doi:10.1051/cocv:1996101.

[55] S. Semenov, J. Kellam, P. Althausen, T. Williams, A. Abubakar, A. Bulyshev, and Y. Sizov. Microwave tomography for functional imaging of extremity soft tissues: feasibility assessment. *Physics in Medicine and Biology*, 52(18):5705–5719, 2007. doi:10.1088/0031-9155/52/18/015.

[56] S. Y. Semenov, A. E. Bulyshev, A. Abubakar, V. G. Posukh, A. E. Souvorov, P. M. van den Berg, and T. C. Williams. Microwave-tomographic imaging of the high dielectric-contrast object using different image-reconstruction approaches. *IEEE Transactions on Microwave Theory and Techniques*, 53(7):2284–2294, 2005. doi:10.1109/TMTT.2005.850459.

[57] S. Y. Semenov, R. H. Svenson, and G. P. Tatsis. Microwave spectroscopy of myocardial ischemia and infarction. 1. Experimental study. *Annals of Biomedical Engineering*, 28:48–54, 2000. doi:10.1114/1.253.

[58] J. A. Sethian and A. Wiegmann. Structural boundary design via level set and immersed interface methods. *Journal of Computational Physics*, 163(2):489–528, 2000. doi:10.1006/jcph.2000.6581.

[59] O. Sigmund. *Design of Material Structures Using Topology Optimization*. PhD thesis, Technical University of Denmark, 1994.

[60] O. Sigmund and J. S. Jensen. Design of acoustic devices by topology optimization. In In C. Cinquini, M. Rovati, P. Venini, and R. Nascimbene, editors, *Short papers of the 5th World Congress on Structural and Multidisciplinary Optimization WCSMO5. Lido de Jesolo, May, 2003, pp. 267–268*, 2003.

[61] O. Sigmund and J. Petersson. Numerical instabilities in topology optimization: a survey on procedures dealing with checkerboards, mesh-dependencies and local minima. *Structural Optimization*, 16(1):68–75, 1998. doi:10.1007/BF01214002.

[62] A. E. Souvorov, A. E. Bulyshev, S. Y. Semenov, R. H. Svenson, A. G. Nazarov, Y. E. Sizov, and G. P. Tatsis. Microwave tomography: a two-dimensional Newton iterative scheme. *IEEE Transactions on Microwave Theory and Techniques*, 46(11):1654–1659, 1998. doi:10.1109/22.734548.

[63] M. Stolpe. Global optimization of minimum weight truss topology problems with stress, displacement, and local buckling constraints using branch-and-bound. *International Journal for Numerical Methods in Engineering*, 61(8):1270–1309, 2004. doi:10.1002/nme.1112.

[64] M. Stolpe and K. Svanberg. An alternative interpolation scheme for minimum compliance topology optimization. *Structural and Multidisciplinary Optimization*, 22:116–124, 2001. doi:10.1007/s001580100129.

[65] M. Stolpe and K. Svanberg. Modelling topology optimization problems as linear mixed 0–1 programs. *International Journal for Numerical Methods in Engineering*, 57(5):723–739, 2003. doi:10.1002/nme.700.

[66] K. Svanberg and M. Werme. A hierarchical neighbourhood search method for topology optimization. *Structural and Multidisciplinary Optimization*, 29(5):325–340, 2005. doi:10.1007/s00158-004-0493-x.

[67] K. Svanberg and M. Werme. Topology optimization by a neighbourhood search method based on efficient sensitivity calculations. *International Journal for Numerical Methods in Engineering*, 67(12):1670–1699, 2006. doi:10.1002/nme.1677.

[68] R. Udawalpola and M. Berggren. Optimization of an acoustic horn with respect to efficiency and directivity. *International Journal for Numerical Methods in Engineering*, 73(11):1571–1606, 2008. doi:10.1002/nme.2132.

Acta Universitatis Upsaliensis
Digital Comprehensive Summaries of Uppsala Dissertations from the Faculty of Science and Technology 612

Editor: The Dean of the Faculty of Science and Technology

A doctoral dissertation from the Faculty of Science and Technology, Uppsala University, is usually a summary of a number of papers. A few copies of the complete dissertation are kept at major Swedish research libraries, while the summary alone is distributed internationally through the series Digital Comprehensive Summaries of Uppsala Dissertations from the Faculty of Science and Technology. (Prior to January, 2005, the series was published under the title "Comprehensive Summaries of Uppsala Dissertations from the Faculty of Science and Technology".)

ACTA
UNIVERSITATIS
UPSALIENSIS
UPPSALA
2009

Distribution: publications.uu.se
urn:nbn:se:uu:diva-98382